Effect of The Liquid Drainage Upon The Rise Velocity Of Large Bubbles In Stagnant Newtonian and Non-Newtonian Liquids (Non-circular channels)

By G. Pena and D.D. Joseph
Department of Aerospace Engineering and Mechanics
University of Minnesota, Minneapolis, MN 55455, USA
April 2002

1. Introduction

The rise velocity of large bubbles in unbounded media and channels has received considerable attention both experimentally and theoretically, but only a few studies dealing with the bubble rise velocity in non-circular channels have appeared. The two-phase flow pattern, usually called “Taylor bubbles”, is encountered when gas and liquid flow simultaneously in a channel, over a certain range of flow rates. The Taylor bubble almost fills the channel cross section and moves upward with a constant velocity, and the liquid moves downward around the bubbles in the form of a film falling under gravity.

This work describes an experimental investigation of the rise velocity of large bubbles through rectangular channels with sections having parallel slices.

The experimental research is presented in two chapters: one using Newtonian fluid and another using non-Newtonian fluids. The main goal of the research is to determine the effects of liquid drainage on the rise velocity.

2. Experimental equipment

The experimental apparatus is a rectangular channel whose cross section is ¼” x 2”, 60 inches high, made of fiberglass. The tests were made for two cases described below as a high (HL) and low (LL) liquid level. Here HL and LL are

related to the height of inserts inside the channel (see figure 1a). We varied the number of inserts and distance between them (see figure 1b).

The Taylor bubbles were formed by injection of air using a piston.

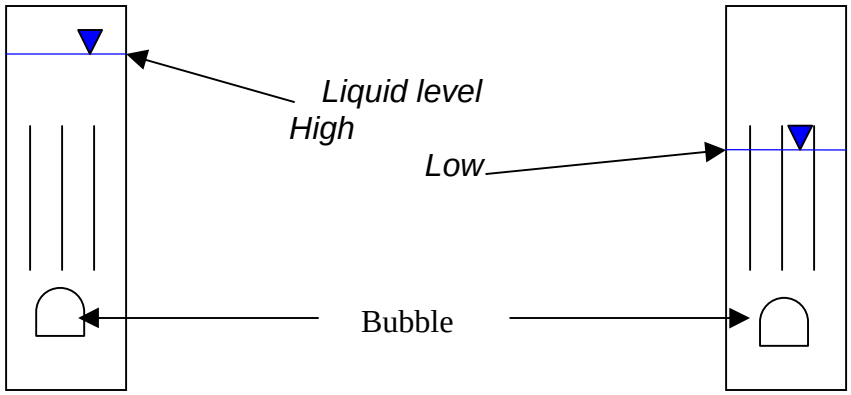

***Figure 1a**. Cases – High (HL) and low Level (LL).*

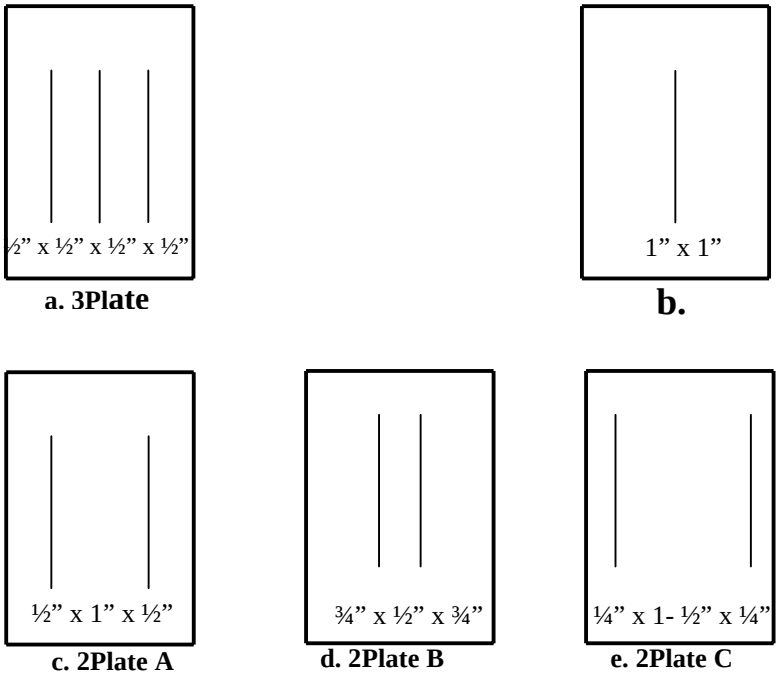

Figure 1b. Inserts in the channel

3. Newtonian liquids.

The experiments were carried out in a number of the tests with glycerin solutions with different viscosities. The glycerin was diluted with water at four concentrations, 75, 60, 40 percent, and plain water

3.1. Rise velocity in a channel without plates.

As the bubble rises, it must displace fluid, which is transported from the nose to the rear of the bubble. Since the pressure in the long part of the bubble is constant, the liquid is on the wall and there is a film falling under gravity. The initial bubble shape can be seen in the figure 2.

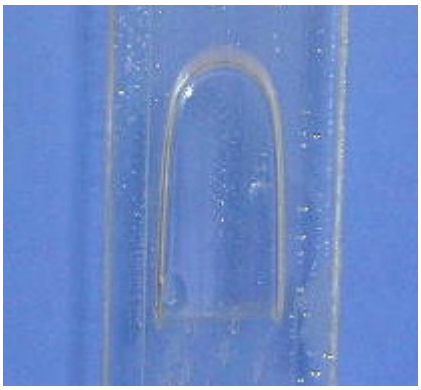

Figure 2. *Taylor bubble shape in the rectangular channel*

The rise velocities obtained during the test, for water (0% glycerin) and 60% glycerin, were nearly constant around values of 178 and 172 mm/s respectively. Dumitrescu [1] used potential flow to predict the terminal velocity of a bubble, using a static liquid in a tube. Taking into account the flow at the nose and in the film he obtains a rise velocity:

$$V_b = 0.35\ (g*D)^{1/2} \qquad (1)$$

Davis and Taylor [2] also obtained the potential flow solution for flow in a tube as did Dumitrescu, but their solution is approximate. Their find:

$$V_b = 0.328\ (g*D)^{1/2} \qquad (2)$$

Brown [3] did an experimental and theoretical study of the effect of the viscosity in the rise velocity. He obtained a correlation, which is in good agreement with experimental results for systems in which the effects of surface tension and liquid viscosity on the frontal flow are negligible:

$$V_b = 0.35\ (g*D)^{1/2}\ *\{1 - [(1+ND)^{1/2} - 1] / ND/2\}^{1/2} \qquad (3)$$

$$N = [\ 14.5*\rho^2 * g / \mu^2\ ]^{1/3}$$

Brown's equation reduces to Dumitrescu for an inviscid liquid, $\mu = 0$.

Zukoski [4] studied the influence of the viscosity, surface tension, pipe diameter, and pipe inclination angle, using the Reynolds number (Re). It was observed that for Re > 200, the propagation rates are substantially independent of viscous effects, and for values $\Sigma < 0.1$ the rise velocity can be predicted by Davis and Taylor equation.

$$\Sigma = \text{Surface tension}/(\rho_l - \rho_g)gR^2$$

In the present experiment using glycerin solutions the viscosity is small enough that Dumitrescu's equation (1) is applicable. However all of these equations described above are applied to the rise velocity in a circular tube. To use ones of these equations for rectangular channels we define D_e to be an equivalent diameter. Only a few studies dealing with the bubble rise velocity in non-circular channels have appeared. Sadatomi [5], suggested using an equi-periphery diameter, which is wetted periphery divided by π. i.e.

$$D_e = ((2*2 + 2*¼)/ \pi)*25.4mm = 36.38 \text{ mm}.$$

Using this equivalent diameter for water case into the Dumitrescu's equation, we obtained the flowing value:

$$V_b = \boldsymbol{k}.(g.\ D_e)^{1/2} \ ; \ \boldsymbol{k} = 0.35$$

$$V_b = 0.35(9810 \text{ mm/s}^2 * 36.38 \text{ mm})^{1/2} = 209.1 \text{ mm/s}$$

The experimental rise velocity was equal to 178.4 mm/s and the theoretical is quit different; therefore, we had to compute a new coefficient ***k*** value in order to correct the equation (1) and reach the experimental values, then the ***k*** coefficient could be computed as:

$$\boldsymbol{k} = V_b / (g.D_e)^{1/2} = 178.4 / 597.4 = 0.299 \qquad (4)$$

Therefore that ours new equation corrected by coefficient ***k*** is:

$$V_b = \boldsymbol{k}\ (g.D_e)^{1/2} \qquad => \qquad V_b = 0.299(g.D_e)^{1/2} \qquad (5)$$

Then, the equation 5 should be apply to compute the rise velocity in rectangular channel, which the geometric sides relation is giving by $D_b / D_s = 8$. Where D_b is

the bigger size and D_s is the smaller one. The next table 1 shows the ***k*** values, which have been determined experimentally for the fluids used on the test.

Table 1. *Coefficients* ***k*** *calculates for the channel*

	Experimental data			***Calculated data***		
Fluid used	Water	40% Glycerin	60% Glycerin	Water	40% Glycerin	60% Glycerin
Velocity V_b (mm/s)	178.4	177.2	172.43	178.4	177.2	172.43
Const. ***K***				0.299	0.297	0.289

The constant ***k*** values have a very small variation equal to 3% for the range fluid evaluated. Therefore, in order to evaluate the effect of the drainage upon the rise velocity, we will use the above ***k*** values calculated for each experimental test. This methodology certifies o fix the base at the same condition to evaluation.

3.2. Rise velocity in 3 plates channel – High Level (HL).

The bubble is going up through the rectangular section. When the nose bubble touches the plates, the initial bubble is divided in four smaller bubbles, figure 3. At that moment the two center bubbles start to increase in velocity and the two outside channels become in drainages channel.

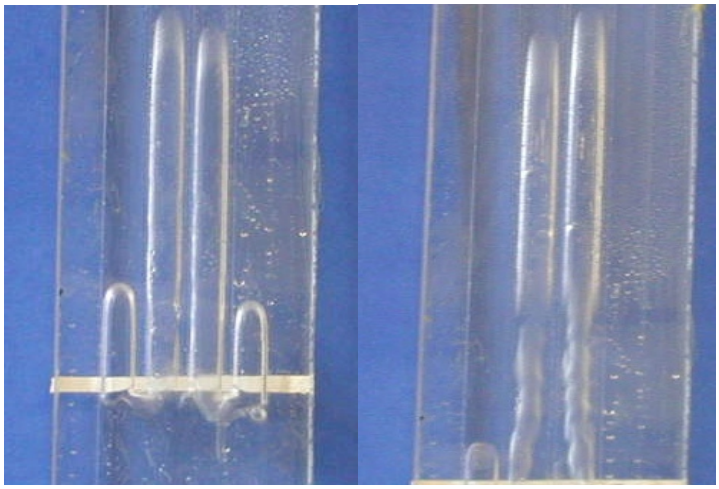

Figure 3*.* The bubbles rise though the three plates channel.

The physic phenomenon can be understood as the presence of the pressure misbalance ahead of the bubble. This pressure misbalance does that the two bubbles take the two central channel, in consequence, the liquid circulation is going down by the two outside channels, increasing the liquid drainage from the two center channels to both outer channels and proportionality the rise velocity is increased too. See the next sketch, figure 4.

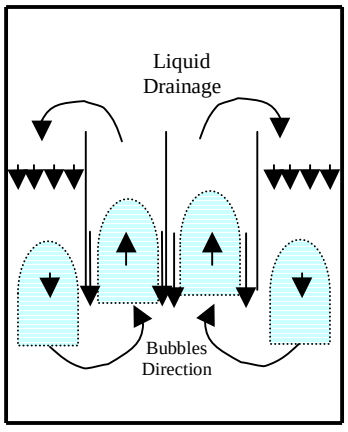

Figure 4*.* Liquid circulation through the external channels – 3Plate

The two external bubbles are going down (negative velocity) to the end of the plates until are joined with the internal bubbles. Therefore, that the four bubbles become in two longer bubbles through the two central channels, see figure 3. For the three plates case we also compute the ***k*** coefficient, which are shown at the next table 2.

Table 2. Coefficient ***k*** calculated for three plates channel - HL

	Experimental data			***Calculated data***		
Fluid used	Water	40% Glycerin	60% Glycerin	Water	40% Glycerin	60% Glycerin
Velocity Vb (mm/s)	396.31	354.64	269.62	205.99	204.61	199.109
Constant ***K*** fixed				0.299	0.297	0.289
New. ***K***1				0.574	0.514	0.391
Ratio Knew/kold				1.924	1.733	1.354

As shown in the table 2., using the same equation 5 with the same constant ***k*** *0.299*, and the equi-periphery diameter (48.51 mm) corresponding to three plates case, the velocities calculated are completely wrong. These suggest that the parameter ***k*** is considerably affected by the liquid drainage induced by the channel geometrical. Re-computing a new coefficient, **k**1, for this geometry the new values are shown in the table 2, which are larger than the previous calculated. In order to demonstrate how the liquid drainage affects the rise velocity, we will analyze the variants two plates (see figure 1b) at the point 3.4 of the present paper.

3.3. *Rise velocity in 3 plates – Low Level (LL).*

In this particular case, the four small channels become in four smalls independent channels (four bubbles). In others words, there is no liquid circulation between channels; each small channel has its own film drainage around the bubble, then diameter will be for one small channel and equal to 12.127 mm. In consequence the rise velocity is slower than the first case (HL) and also is slower than the rise velocity of initial bubble (rectangular channel) because the film drainage is less than these two cases.

The more important observations respect to this case (LL) and HL studied above are: If we apply the same equation for the cases HL and LL, the values calculated have to be closer but this is not true.

1. The channel geometry no changes between HL and LL.
2. The physical properties of the fluid are the same, not changes.

However the experimental values are completely different of the predicted velocity, as show at the next table 3. Therefore, an others parameter ***k*** has been needed and severely smaller as 0.229 for water, 0.229 and 0.215 for 40% and 60% glycerin respectably, just moving the liquid level into the channel. These observations emphasize the dependence the ***k*** parameter of the liquid drainage.

Table 3. *Experimental versus calculated – three plate LL**.***

	Experimental data			***Calculated data***		
Fluid used	Water	40% Glycerin	60% Glycerin	Water	40% Glycerin	60% Glycerin
Velocity Vb (mm/s)	79.1	79.0	74.34	206.0	204.6	199.11

3.4. Rise velocity through the two plates channel.

The results are quit interesting because the initial bubble rise through the channels as the figure 5 shows. For case 2 Plate A and C, the two outside channels becomes in draining, and for 2Plate B, the initial bubble becomes in two bubbles through the outside channels and the center channel become in liquid draining.

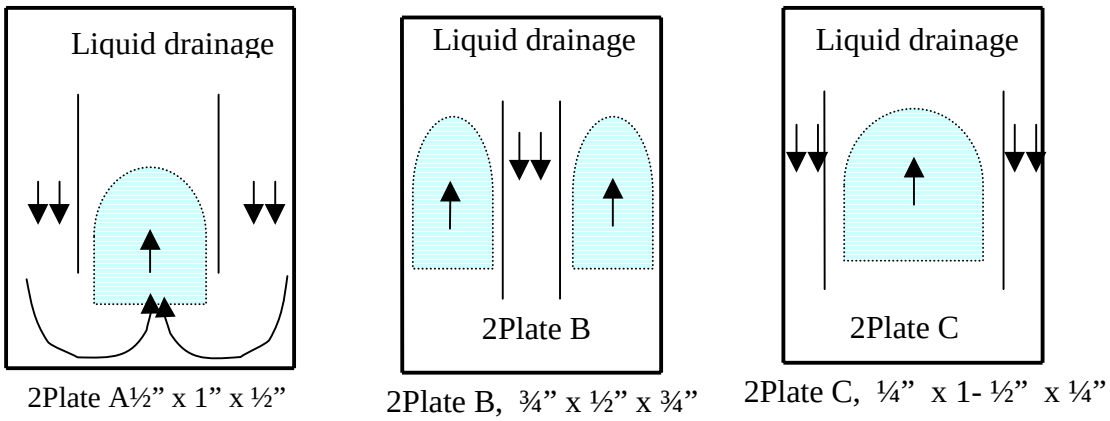

Figure 5. *Develop bubbles rise through 2 Plate channels.*

The Figure 5, show the variants evaluated for this case. We were fixed the equivalent diameter in 1 ¾ in. (D_e = 44.47 mm), and of course the physical properties of the fluid. Therefore, that the velocity is only dependent of the liquid level in the channel and the gap between the inserts for draining.

With this information we did a parametric figure, which related the ***k*** parameter calculated (equation 5) versus the gap, which is the space between the plate and the channel wall. These values are valid for low viscosities liquid between 1 cP

for water and 10 cP for Glycerin 60%. The figure 6 shows the liquid drainage effect upon the bubble velocity in terminus of ***k*** factor.

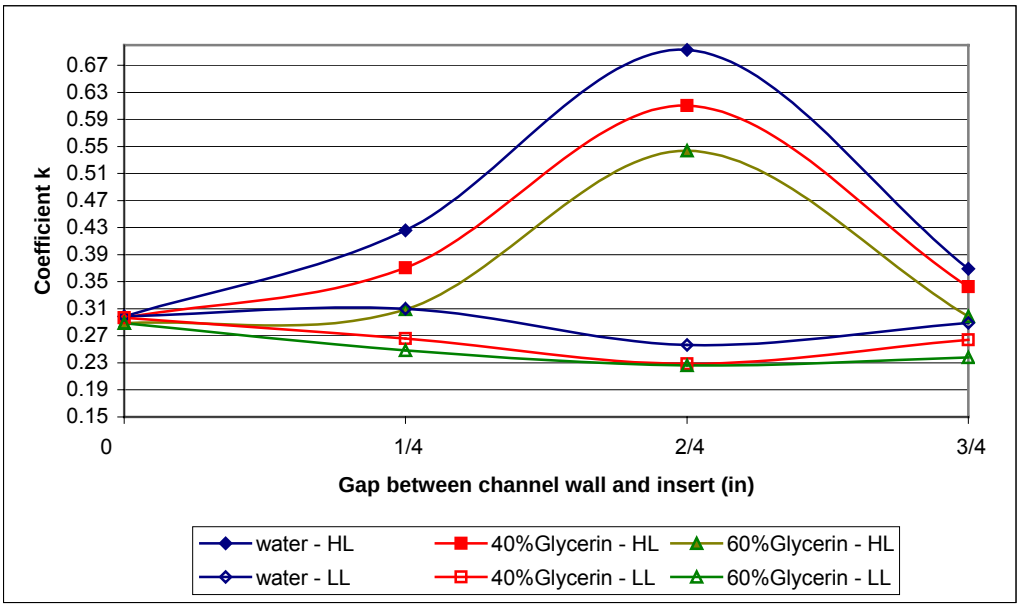

Figure 6. *Effect of the liquid drainage upon the rise velocity*

Analyzing the velocity performance studied above with others predictive velocities methods, we obtains:

- Brown's equation (3): Depend of the liquid viscosity, liquid density and the equivalent diameter. In ours case these three values are constants. If we apply this equation the values obtained is equal to 231.2 mm/s, which is significantly less than the experimental values, the experimental values using water for example are 243.94 mm/s, 281.44 mm/s and 457.66 mm/s as the figure 7 shows. Then, this equation does not take in consideration the liquid drainage effect.
- Zukoski's equation: Depend surface tension number Σ, and Reynolds number Re. In our case, Σ is constant, because the physical property σ it

does not change, and Re is function of the rise velocity, which in HL cases Re increase with the liquid drainage effect; therefore, the factor f(Re) in the Zukoski's equation is going to one when Re≥100. We reach Re ≥ 200. Then the value calculated is 216.7 mm/s, which is also a wrong value.

- Wallis's equation: It is function of Eötvös number Eö, which is based in physical properties, the inverse viscosity number Nf, which is also based in physical properties, and the equivalent diameter. The maximum ***k*** value reached by the wallis's equation is 0.345 (227.9 mm/s). Ours case above studied reach ***k*** values close to 0.7, see figure 6.

Therefore, the equations above decrypted are not applicable for predicting the rise velocity in rectangular channel with inserts. In order to predict the rise velocities with liquid drainage effect the equation of parameter ***k*** is needed. For low viscosity liquid (less than 11 cP) the k values have to be read in the figure 6.

The figure 6 could be apply for rectangular channel with inserts inside and the geometry relation D_e (channel) / D_e (inserts) = 0.82, where gap is the distance between the wall and plate in inch. And the equation 5 can be applied for rectangular channels.

For the cases LL, the factor ***k*** has few variations, but representative in velocities, the range of variation are between 0.309 and 0.248 respectably for extremes fluid evaluated.

The next figure shows the experimental test concerns to the rise velocities versus the drainage gap between the wall of the channel and the plates, variant 2Plate. The results are shown in the figure 7.

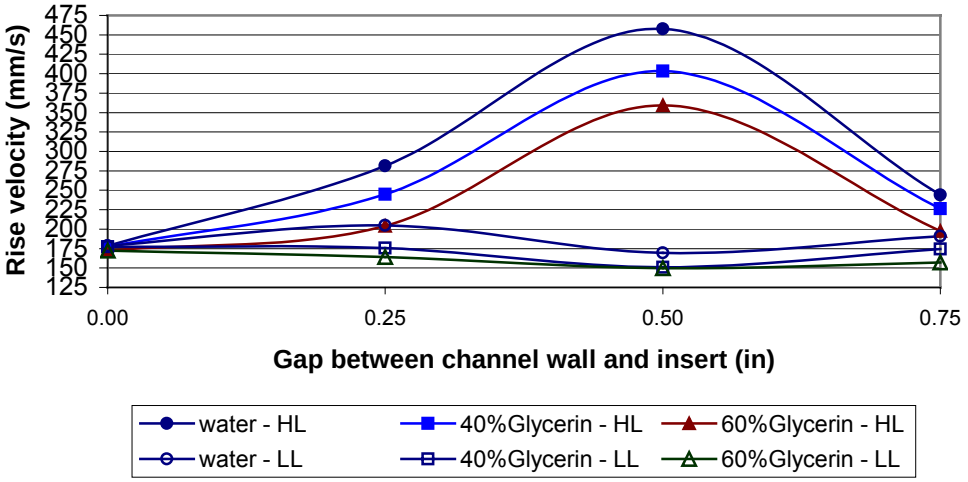

Figure 7. Liquid drainage effect upon the rise velocity – 2Plate

3.5. Rise velocity through *1 plate, cases HL and LL.*

This variant was made with just one plate in the middle of the channel. The big bubble is divided into two bubbles of identical size and rise at the same velocity. Therefore, in 1Plate variant do not exist pressure misbalance mechanism; in such sense, the channels never become for draining. In consequence the liquid level do not influence the rise velocity and the symmetrical bubbles have a symmetrical drainage film, see figure 8.

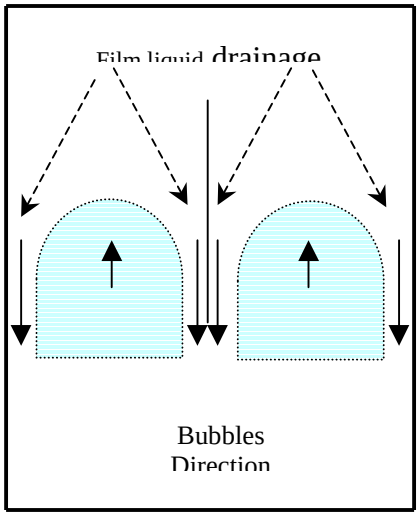

Figure 8. The initial bubble becomes in two bubbles – 1Plate

The table 4 shows the results of the rise velocity tests from 1Plate (De = 40.43 mm); both cases (HL and LL) have the same value by the effect of the symmetry explained above. We can see that the rise bubble velocity (1Plate) is slower than the velocity in the channel. The results are shown in the table 4.

Table 4. *Results obtained in 1 Plate channel HL = LL*

	Experimental data			***Calculated data***		
Fluid used	Water	40% Glycerin	60% Glycerin	Water	40% Glycerin	60% Glycerin
Velocity Vb (mm/s)	127.00	126.60	120.70	188.05	186.79	181.76
Const. K new				0.202	0.201	0.192

The results shown in this case are very important, because confirm our theory about the liquid drainage. In this case it does not have liquid drainage effect, induced by misbalance pressure, in consequence the velocity has the same values for HL and LL. In addition, the not existence of the drainage effect makes insufficient the film liquid downward around the bubbles, which affect is proportionality upon the rise velocity.

4. Experimental research using Non-Newtonian liquid.

The experiments were carried out using the same geometry channel as the test before; but using a liquid with different rheological properties. The liquid used was 1% of Polyox solution, which is viscoelastic fluid.

4.1. Channel without plates.

We are in presence of air bubbles rise through liquids of higher viscosities, therefore, that the hypothesis of potential flow becomes questionable and switch

to creeping flow. The terminal velocity of a rise gas bubble is determined by a balance of weight and drag. For creeping flow, the drag is proportional to V*d and the buoyancy to d^3; hence V is proportional to d^2 in creeping flow. Therefore, the only way to increase the bubble velocity is to increase the bubble volume.[10]

The bubble shape is shown in the figure 9. When an air bubble rises in a viscoelastic fluid, the form at the tail looks like a smooth edge, and the nose takes a spherical shape. The measured velocity through the channel was 106.5 mm/s. Also, we can see that the liquid film is very wide, almost fills half cross section channel.

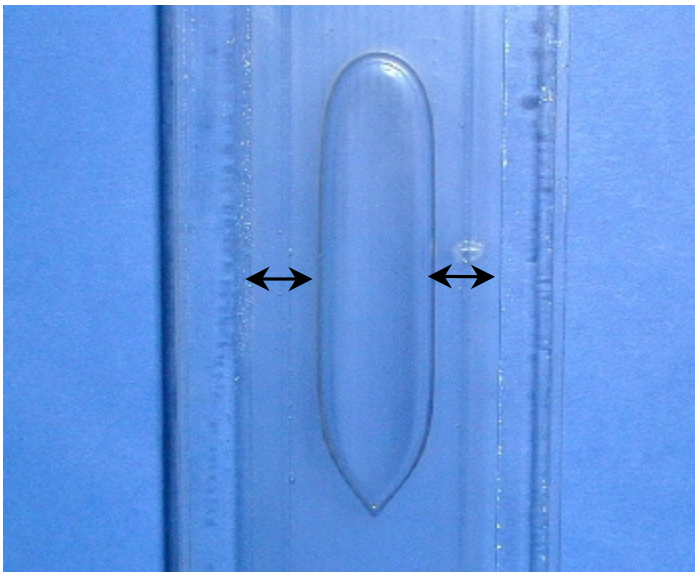

Figure 9. *Bubble rise in a viscoelastic fluid in rectangular channel*

The reduction of cross-sectional area available to the gas at higher liquid viscosities can be explained by a theoretical consideration of the change in pressure with elevation in the region of gas slug. The pressure in the gas phase, a distance equal to the length of the bubble is giving by the weigh of the bubble plus the pressure on the nose. Similarly, the pressure in the liquid phase at the

same elevation is given by the weigh of the liquid column plus the pressure on the nose minus the frictional pressure. If the capillarity forces are negligible for the channel diameter involved, the pressure in the liquid and the gas must be the same at the same elevation. Combining these two relations and solving for the viscous pressure gradient in the liquid yields:

$$\Delta p_f / \Delta L = c(\rho_L - \rho_g) \qquad (6)$$

where c is a unit conversion constant.

The viscous pressure gradient in the liquid backflow region depends only on the density difference between the two phases. Thus, if the liquid phase viscosity increases, the area of the liquid backflow region must also increase, so that the viscous pressure loss remains constant.

4.2 Channel with three pates

The big bubble is divided in four smaller bubbles, figure 10. The four bubbles rise at the same velocity each ones, 17.2 mm/s for HL, and 16.8 mm/s for LL. The velocities are 6.19 times approximately slower than the channel velocity. Therefore, that the liquid drainage found more restriction to falling down by the plates, and the relative value of the liquid film is also reduced. This physical phenomenon could be attributed at the surface tension effect generated by the relative reduction of the cross section. Then the capillary effects of surface tension became significant in this case.

The two cases, HL and LL, are almost the same velocity value, which means that the no channel is become in liquid drain. In others words, there is no circulation

between channels; each small channel has its own film drainage. Graphically can be seen at the next sketch, figure 10.

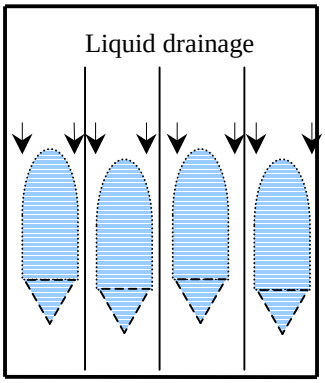

Figure 10. Four bubbles rise at the same velocity – 3Plate

4.3. Channel and one plate – 1Plate.

In this particular case, the big bubble becomes in two bubbles, both bubbles rise at the same velocity, 60 mm/s, even for HL and LL. (See figure 11). The velocity increased about 3.53 times respect to the 3Plate case. Which means that the total film drain area for one plate is bigger than the total film drain area for three plates; but less than the channel (velocity equal to106.5 mm/s). There is no liquid circulation between channels; each channel has its own film drainage.

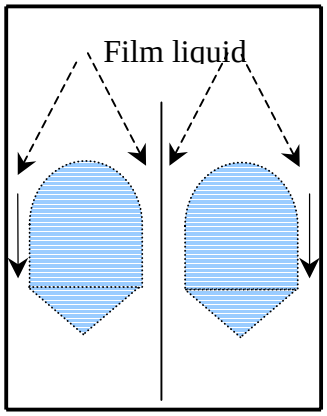

Figure 11. Results 1Plate – Rise velocities of the bubbles

4.4 Channel and two plates.

The bubbles rise formation are the same as the Newtonian case, see figure 12, but rise with the following velocities in mm/s:

Table 5. *Rise velocities through 2 Plate channels*. (mm/s)

Liquid Level	Case A	Case B	Case C
HL	71.8	58.2	87.6
LL	66.0	54.5	81.0

The difference between HL and LL shown in the table 5, Identify that exists a little liquid drainage through the channels, see figure 12.

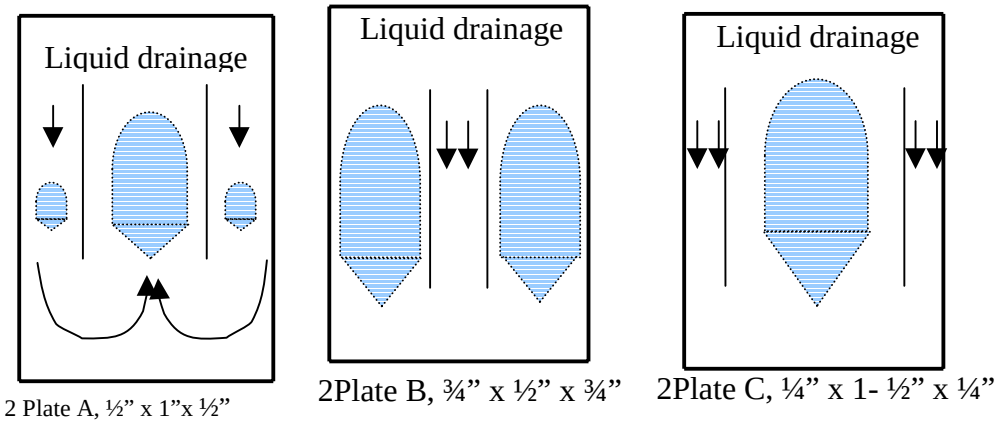

Figure 12. Liquid drainage – 2 Plates channel.

The more important situation is the formation of two small bubbles (2 Plate A), which partially plug the falling liquid in both sides for HL case. However, the liquid drainage exits through the outside channels. For the LL case, the three bubbles rise at the same velocity. The next figure 13 shows the comparative behavior of the liquid drainage effect upon the bubble velocity.

The liquid drainage for viscoelastic liquid is strongly dependent of the space between the plates and the wall. This effect is attributed for the interface tension generated between plates and the fluid.

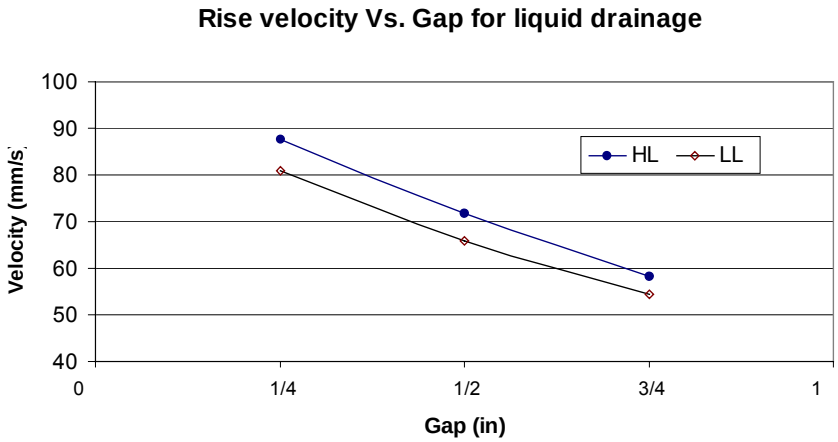

Figure 13. *Comparative liquid drainage effect*

The velocity increase is the gap decrease; therefore, if plates are eliminated the maximum velocity is reached, which is the channel velocity equal to 106.5mm/s. The figure 14 shows the comparative behavior velocities for all cases evaluated. The maximum velocity is for the channel and the minimum velocity is for three plate's case.

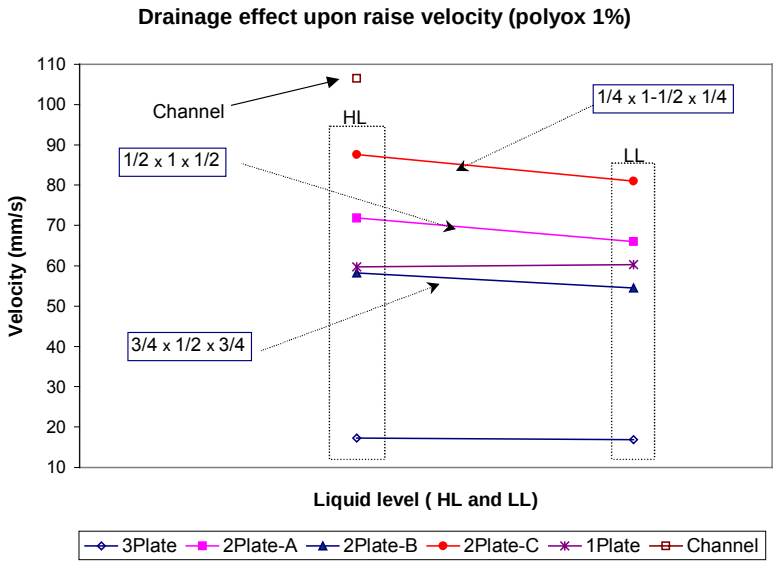

Figure 14 *Comparative cases evaluated*

5.*CONCLUSION.*

During this experimental behavior we studied and shown that the rise velocity is influenced by the liquid drainage, specifically in noncircular channels. It should be pointed out that the present detailed study and observations of the how the rise velocity can be affected by drained liquid has never been addressed in the existing literature. To predict the bubble rising velocity in the noncircular channels with inserts, a new theory needs to be developed.

There are many industrial applications, but the mayor could be the oil industry by producing natural gas, specifically in the kind water–gas or water-condenser-gas reservoirs.

5.1 Newtonian fluid

The experimental study determined an important factor affecting the velocity of the bubbles rise in rectangular channels. This factor is called liquid drainage. The dependency between the drainage and the bubble velocity are directly proportional. Also the research shown that a pressure misbalance in from of the bubbles in the channels, make influence to become some area for liquid circulation or drainage, thus increasing the rise bubble velocity in 2.57, 2.27, and 2.08 times for the cases water, 40%glycerine, and 60%Glycerine respectability. Therefore, this work show how the gas velocity may be increased, without changes in the cross sectional area of the channels.

There are not methods to predict the bubble rise velocity through rectangular channels in presence of the liquid drainage. The present approach provides a reasonable data in order to correct the factors calculates by knowing predictive method for the rise velocity in rectangular channels.

5.2 Non-Newtonian Fluid.

The rise velocity is strongly dependent on the gap for liquid film drainage; because, surface tension force is increased when the gap is reduced, like capillary phenomena. The research shown that a pressure misbalance by the liquid level is not makes a big influence to become some area for liquid circulation or drainage. Thus for viscoelastic fluid, the faster rise bubble velocity is reached when the minimum restriction for the liquid drainage exist.

REFERENCES.

1. Dumitrescu, D. T.: (1943). “Stromung an einer Luftblase in senkrechten Rohr” ZAAM. 23, No. 3, 139 – 149.
2. Davis, R. M. & Taylor, G. I. (1950). The mechanics of large bubbles rise through extended liquids and through liquids in tubes. Proc. Roy. Soc. 200, Ser. A, 375 – 390.
3. Brown, R.A.S (1965). The mechanics of the large gas bubbles in tubes. The Canadian J. of Chem. Eng. V, 43, 217 – 223.
4. Zukoski, EE (1966). Influence of viscosity, surface tension, and inclination angle on motion of long bubbles in closed tubes. J. Fluid mech. V.25, 821-837
5. Sadatomi M., Sato Y., and Saruwatari S. (1982). Two – Phase flow in vertical noncircular channels. Dep. Mechanical Engineering Kumamoto University and Ariake technical collage Omuta Japan. 641 – 653.
6. D. Barnea and L. Schemer (1986). Rise velocity of large bubbles in stagnation liquid in non-circular ducts, Int. J. Multiphase flow. V. 12, No. 6, 1025-1027.
7. Q.C. Bai, T.S. Zhao (2001). Taylor bubbles in miniaturized circular and noncircular channels. International Jornal of Multiphase Flow 27, 561-570.
8. V.C. Kelessidis and A.E. Dukler (1990), Motion of large gas bubbles through liquids in vertical concentric and eccentric annuls. Int. J. Multiphase Flow. Vol. 16. No. 3, 375-390

9. D. W. Rader, SPE- AIME. Sun oil Co. (1975). Factors affecting bubble-rise velocity of gas kicks.
10. Y.J.Liu, T. Y. Liao and D.D Joseph (1995). A two-dimensional cusp at the trailing edge of an air bubble rise in a viscoelastic liquid. J. Fluid Mech. Vol. 304, 321-342.

Drag Coefficient Determination in Partly Boundary Media (Internal Flow)

By Gilberto Pena, D.D. Joseph
Department of Aerospace Engineering and Mechanics
University of Minnesota, Minneapolis, MN 55455, USA
April 2002

4. Introduction

Whenever an object is placed in a moving fluid (or moves through a stationary fluid) it will experience a force in the direction of the motion of the fluid relative to the object (drag force, D). This force may be expressed as:

$$D = C_D(\rho V^2/2)A \qquad (1)$$

Hence ***A*** is the characteristic area which usually the surface area or the projected area normal to the flow direction. The equation (1) defines the drag coefficient C_D. In all except few cases this coefficient must be experimentally determined, and they generally depend on the Reynolds number.

The drag force is caused by the sum of the tangential and normal forces at the surface of the body. The drag due to tangential stress is variously called friction drag, skin friction drag, or viscous drag. This kind of drag is most important where the surface area parallel to the flow direction is large compared to the projected area normal to the flow. For example, skin friction drag accounts for all of the drag on a flat plate aligned with the flow.

The drag due to normal stresses is called form or pressure drag. Pressure drag is more important and often dominant for bluff bodies. Also, for an internal flow another important physical phenomena appear, which is the boundary layer. The

uniform stream velocity accelerates as the boundary layer grows, then the drag due by tangential stress took an important place in this kind of flows.

In order to determine the total drag coefficient for internal flow, we did an experimental research in a vertical pipe system using different particles shapes.

5. **Experimental equipment.**

The experimental apparatus is a vertical circuit build with fiberglass 1 inches pipe diameter. The fluid is moved by centrifugal pump and the flow rate is controlled by a set of valves and monitored by a flow meter, the system has a particle shuttle chamber, figure 1.

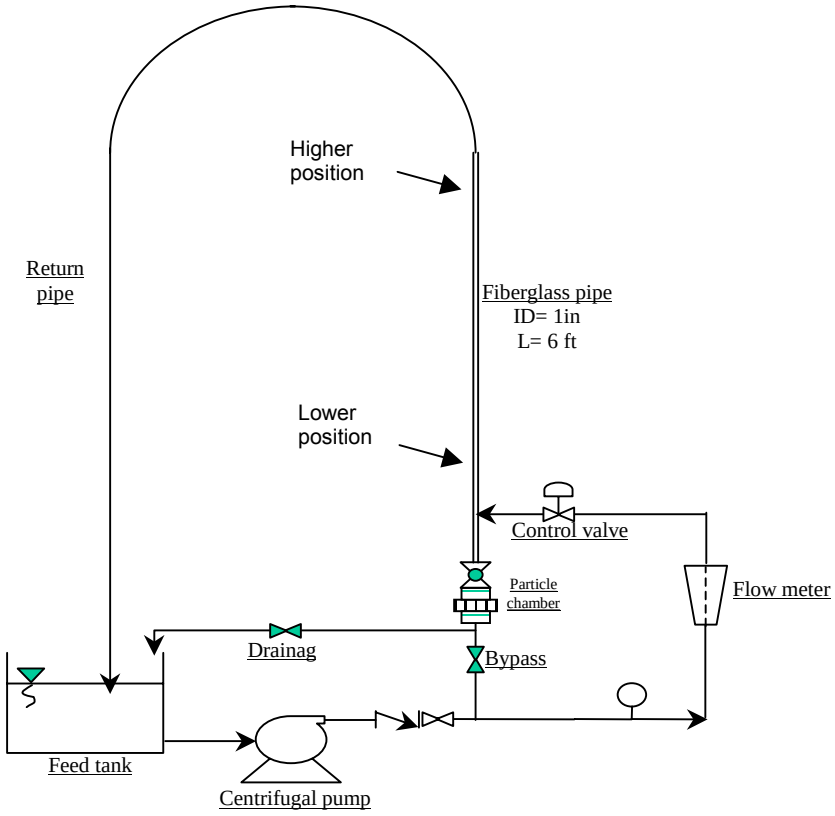

Figure 1. Schematic of the circuit test

The first part of experimental test was made using three forms (a, b, and c) of particles with different diameters made of Teflon (ρ = 2154 Kg/m^3), as: spherical and flat face cylinders ½, 5/8, and ¾ in diameter and spheres ½ and ¾ inches diameter, figure 2. And also we tested the arrow shape, figure 2 (d), we were working with ½, 5/8, and ¾ in diameter made in aluminum (ρ = 2827 Kg/m^3), each of ones with the same weight.

The second experimental part was focused on not conventional shapes, which can be adapted by a robot itself called “Columbus”, figure 3. This robot is a prototype device which will be send to the well production oil in order to know some properties precisely as pressure, temperature, density, etc., the robot position will be manipulated adjusting the cross section area. Therefore, our main goal is to know how the drag coefficient vary in function of the ratio cross-section area and the more important to know the hydrodynamic stability. The replica was made in aluminum, figure 4.

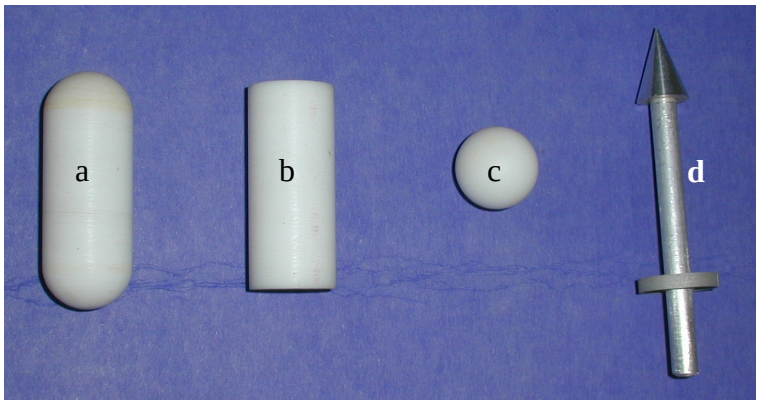

Figure 2. Particles shapes used during the test

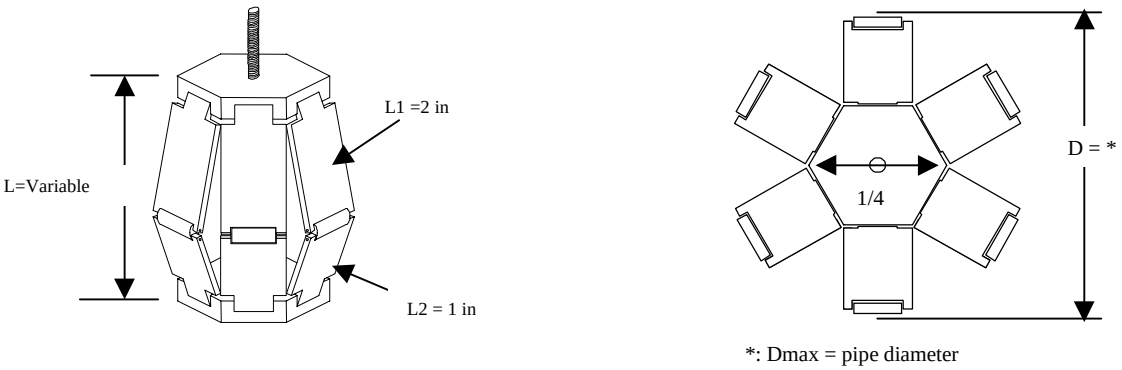

Figure 3. The actual Columbus shape

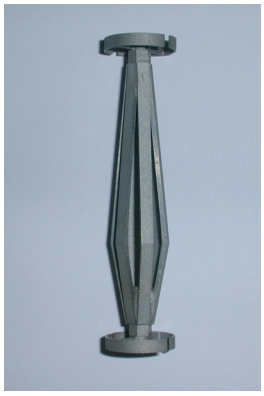

Figure 4. Columbus head shape replica

6. Result obtained.

The results were obtained applying the balance equation, which relates the drag force, the buoyancy force an the weight, gives:

$$F_D = W - F_B \qquad (2)$$

F_D is the drag force, W is the particle weight, and F_B is the buoyant force, which is equal to the unit weight of the fluid multiplied by the volume of the particle, then using the equation (1) and (2):

$$C_D(\rho V^2/2)A = (W - F_B)*g$$

Or

$$\therefore \quad C_D = [(W - F_B)*g]/[(\rho V^2/2)A] \qquad (3)$$

The figure 5, shown the C_D values obtained for the shapes a, b and c. As was explained above, the drag coefficients for partly internal flow are expected bigger than the C_D published in the literature, which correspond to external flow. For example for flat faced cylinder Re > 10^4 and L/d = 4, the coefficient is C_D = 0.87 for external flow and our case, for the same condition C_D = 1.92, which is 2.2 time bigger one.

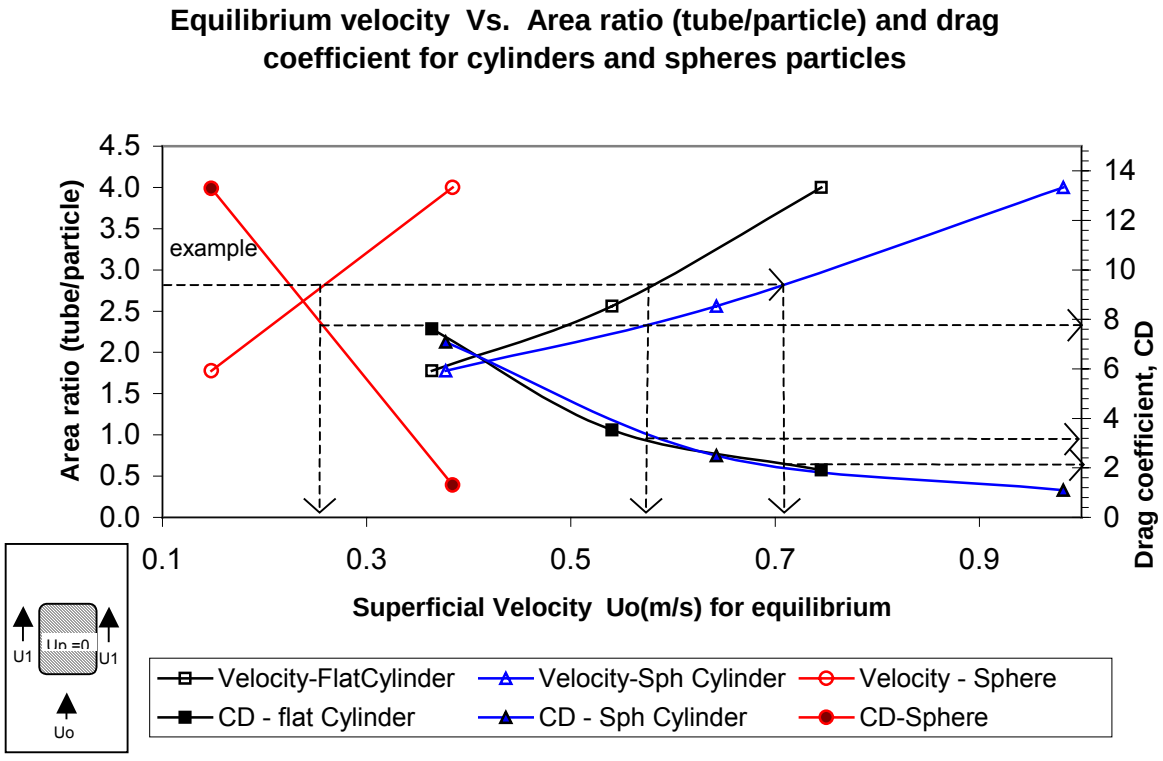

Figure 5. Drag coefficient for internal flow

In order to present the data easy to read, we present the coefficients of the figure 5 in the next table 1.

Table 1. Drag coefficient for internal flow

Particle	Area ratio (At/Ap)	Velocity Uo (m/s)	CD
Spheres	4.00	0.384	1.30
	1.78	0.148	13.29
Flat-	4.00	0.745	1.92
Cylinders	2.56	0.540	3.54
	1.78	0.364	7.62
Sph -	4.00	0.982	1.10
Cylinders	2.56	0.642	2.49
	1.78	0.377	7.08

All of the cases presents above the drag coefficient are bigger than the values knows for external flow, especially for the sphere ¾ inches case C_D = 13.29 vs. 0.4. This incremental effect can be explained by the increase of the annular velocity ***U1*** *(*annular velocity), which is proportional to the skin friction drag or tangential forces.

Therefore, when we are in presence of unbounded systems the equilibrium velocity ***Uo*** is equal to ***U1*** and the addition of skin drag is not the more important value, but in ours case we have ***U1*** > ***Uo*** between values 1.3 to 2.3 times bigger, then the tangential force becomes in an important effect.

Additionally, another important observation resulted from this study. The equilibrium flow rate, particle velocity equal to zero, is function of the position of the particle into the tube; the evaluated positions (lower and higher) are shown in the figure 1. We defined the equilibrium position as the stable performance or smooth waving, see figure 6.

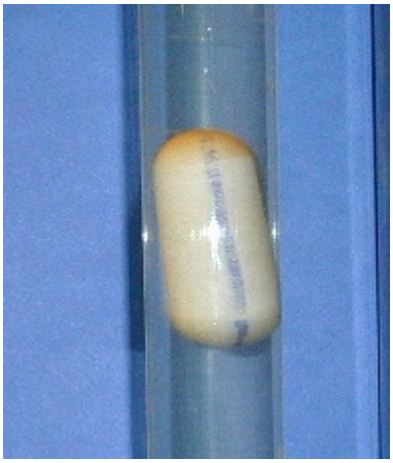

Figure 6. Equilibrium particle position

For the lower position the equilibrium flow rate is bigger than the higher position, see table 2.

Table 2. Particles position vs. Equilibrium flow rate

Cylindrical Particle	Lts/min (Lower position)	Lts/min (Higher position)	Variation (%)
¾ x 1.8 inches (sph)	11.5	10.2	13
¾ x 1.8 inches (flat)	10.6	9.9	7
¾ x 1.5 inches (flat)	8.6	7.9	8.8

The result shows differences of 13% to 7% between two positions. An explanation for this observation is for sure that the hydrodynamic phenomenon is changing between both positions. If the drag coefficient not change and the particle weight neither change, then the equilibrium velocity must be the same in both positions. Therefore, as the flow rate is reduced, the equivalent diameter has to be reduced as well in order to get the same velocity. This diameter

reduction could be attributed by the growth of the boundary layer, which makes to change the hydrodynamic performance.

In addition an instability hydrodynamics was observed, which makes that the particle start to swing horizontally (twisting) and losing the equilibrium position, figure 7, in fact, this instability makes rise the particles with less flow rate than the equilibrium flow. Particularly, this phenomenon hydrodynamic was observed in the particles ¾ in diameter (Tube diameter one inch).

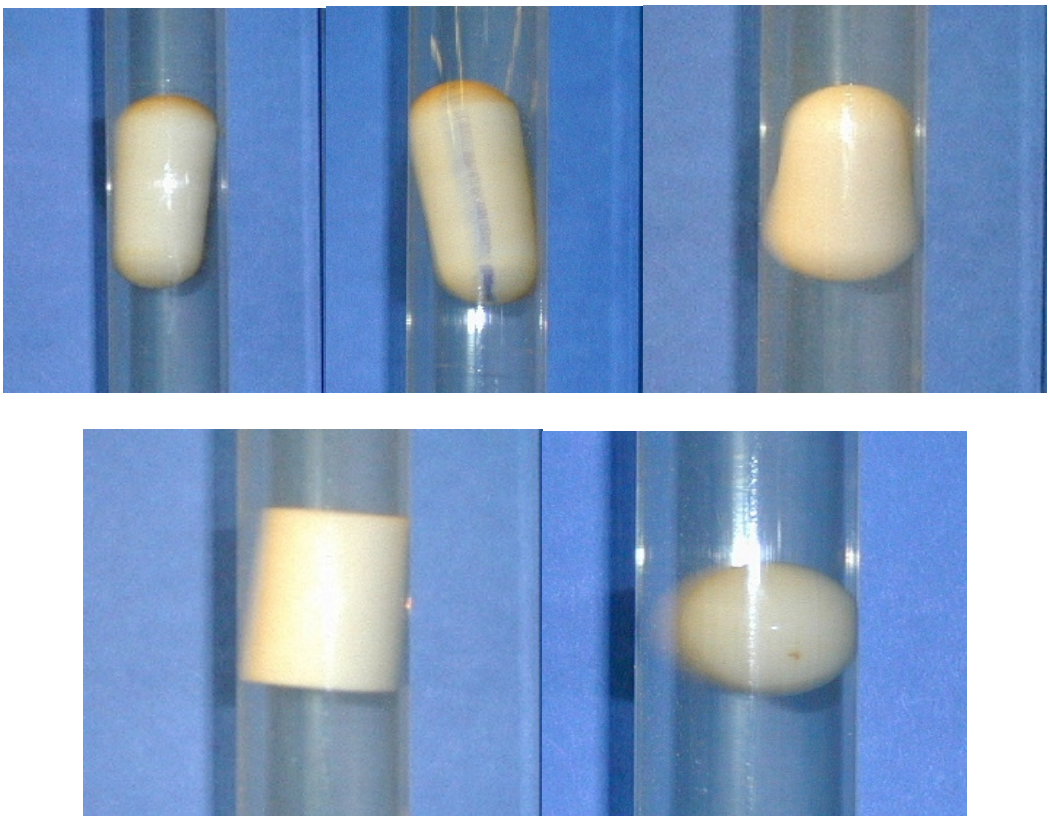

Figure 7. Instability hydraulic - swing

Using particles ½ in diameter the instability does not appear and the equilibrium position is clearly close to wall pipe, figure 8.

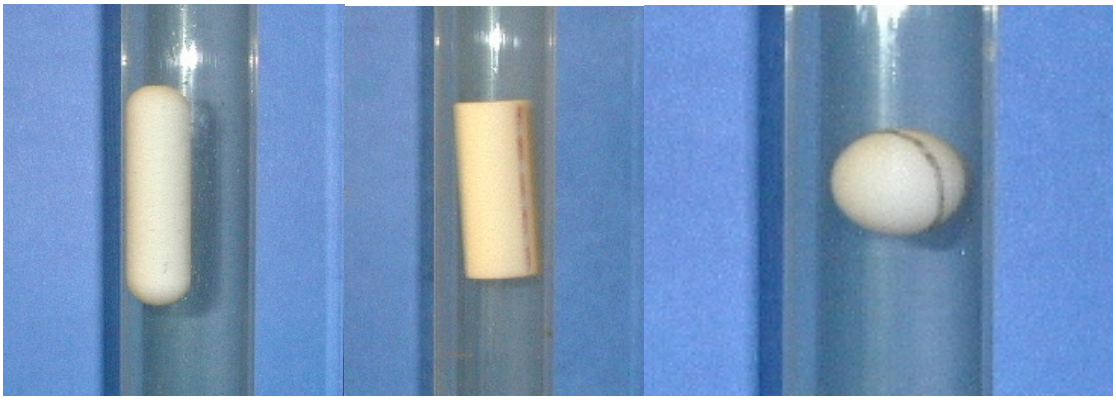

Figure 8. Equilibrium reached close the wall pipe

The position reached by the particles, figure 8, is going to be the zone with less instability than the center of the pipe, which is the reason why the particle rests in that zone. In consequence, the drag coefficient is less than if it was at the middle of the pipe, because the flow velocity close to the wall is less than the center line velocity. Using the particle shape d, figure 2, we have to put an o-ring in order to centralize the particle and maximize the drag coefficient and the results are presented in the figure 9.

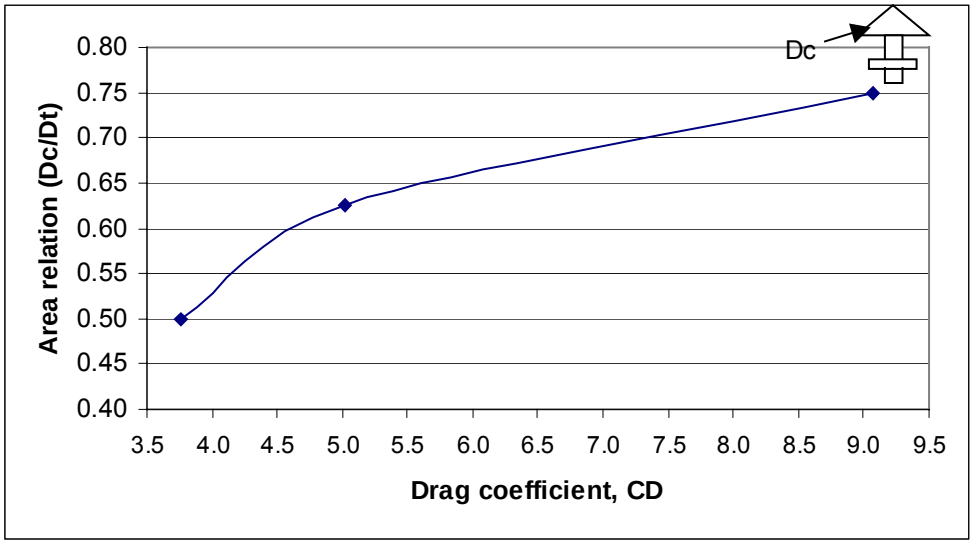

Figure 9. Drag coefficients for arrow shapes.

The figure 9 shows how the drag coefficient grown rapidly with the area ratio, in others words, the incremental percent in C_D by the first step was 26% and by the second step was 45%, each step has the same differential ratio area.

6.1 Results of the second part, Robot "Columbus" tests.

The robot has to have rings to be centered in the tube, as the figure 10 shows, which force the robot to be into flow stream and maximize the drag.

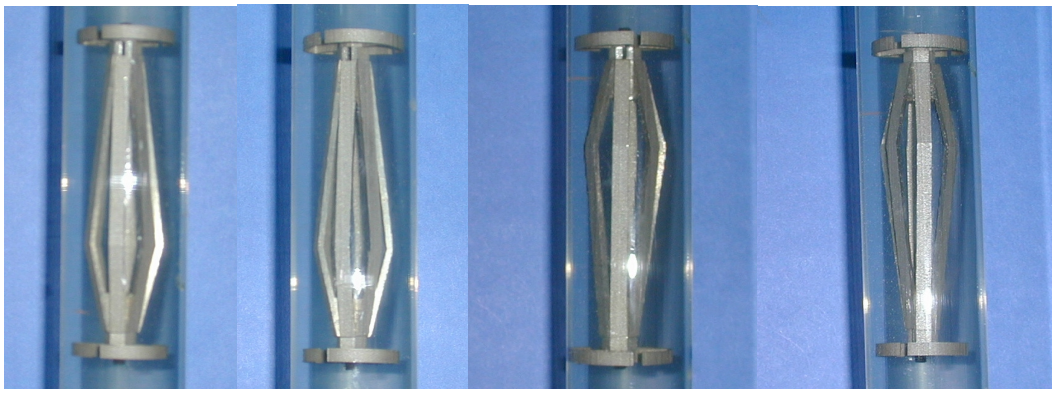

Figure 10. Robot centered by rings – 7,37 grams weigh

Otherwise, the robot will be positioned at the wall of the tube and the drag coefficient will be loosed dramatically. The figure 11 shows how the robot will be positioned without the rings.

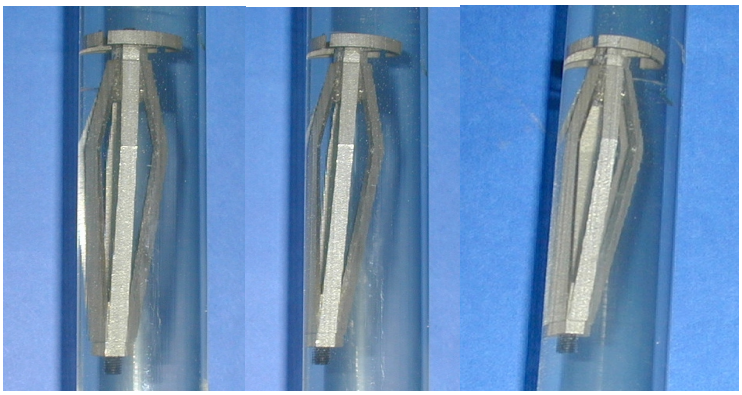

Figure 11. Robot out of the center

Another important test was made, which consisted to flip it vertically (figure 12), compute the drag coefficient in both case, and observe the stability changes. Using diameter " d " 0.612 inches, we found that the drag coefficient can be increased 7% (2.84 to 3.04) if the robot is flipped, figure 12, and the stability also is better.

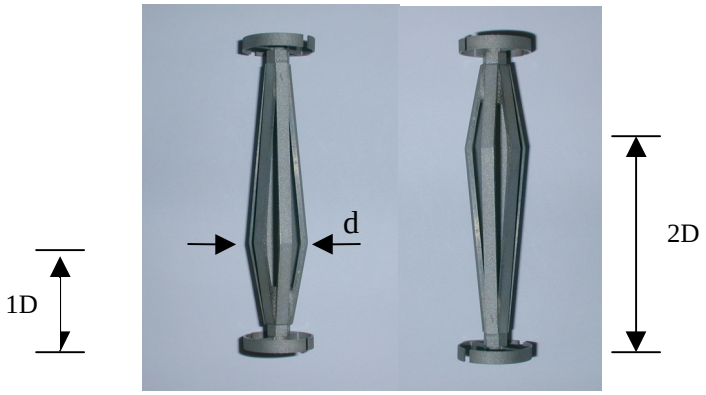

Figure 12. Robot flipped vertically, the left figure is the original ones

The C_D incremental is caused by the tangential forces at the surface of the body. The drag due by the tangential stress or skin friction drag is most important when the robot is flipped, because the first segment of surface area parallel to the flow direction is large compared to the original position. We can think that the separation is present through the pass of flow between two segments with Reynolds number 32000.

In order to evaluate the increment in C_D between both position, we build a robot with dimension shape vary. We can increase or reduce the diameter Dc (***d)*** as the real robot will do, figure 13.

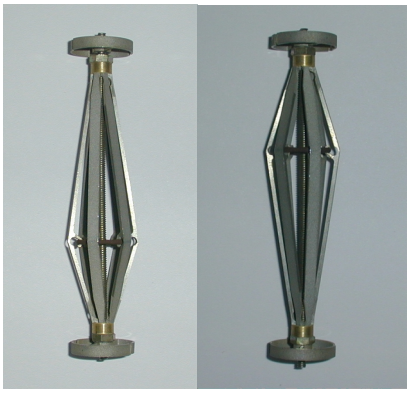

Figure 13. Robot with diameter manually manipulated - 10,3 grams weigh

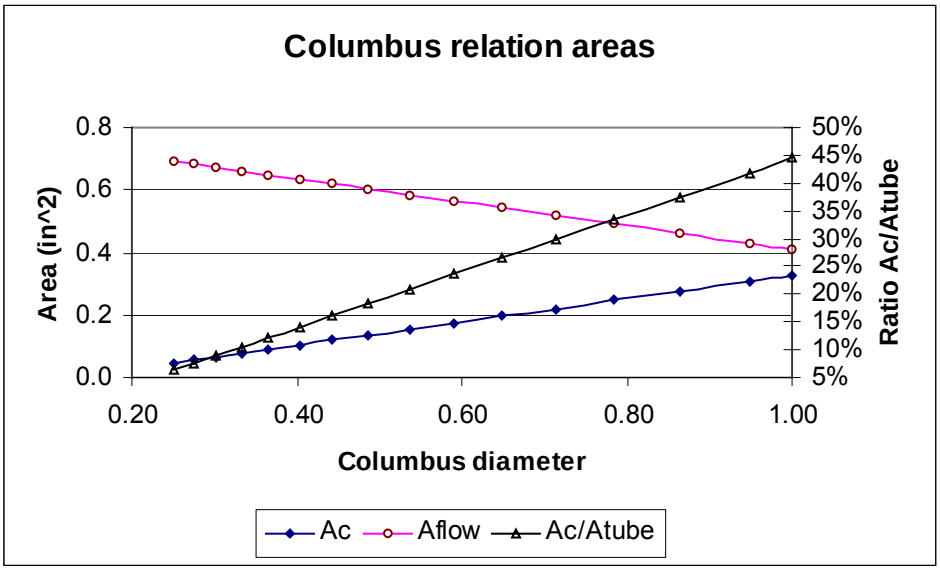

Figure 13a. Operative Columbus area relations

The figure 13a shows the relation areas between the Columbus and pipe, these relations constitute the real operative zone for the robot. Therefore that the Columbus always will operate below 45% of transversal area of the pipe.

The test was based in found the equilibrium position for each case, original and flip. The results are quit imports because we found the incremental C_D in function of the diameter ratio (robot/tube) for both cases, figure 14.

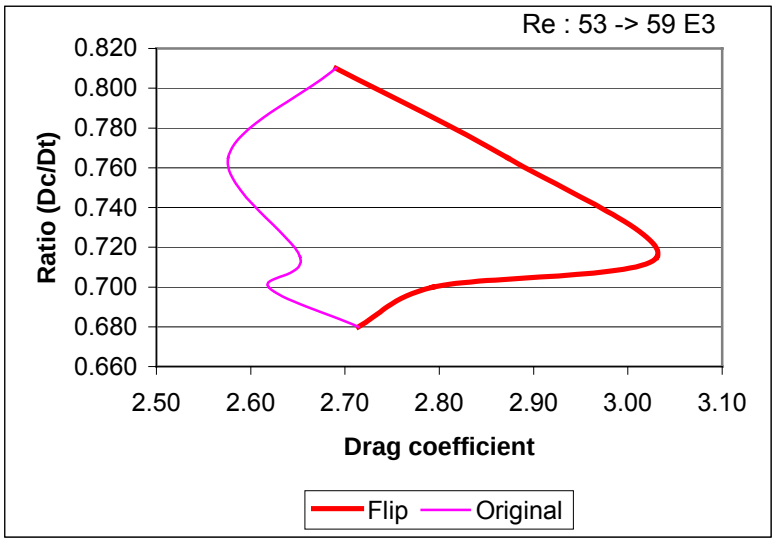

Figure 14. Drag coefficients variation, both cases. $0.27 \leq Ac/At \leq 0.33$

The figure 14 shows the results of the simulations driving robot. We can see that exist a maximum C_D value is for the flip position, this value is 12% bigger that the original position (Dc/Dt =0.71), which is extremely important for the reservoir production oil. This performance is attribution of the skin drag, which plays an important roll upon the total drag force. Also the figure 14 shows that the C_D difference between both cases disappear for $0.68Dt \geq Dc \geq 0.81Dt$, (full closed ≈ full opened). The hydrodynamic clearly shows the drag reduction after a maximum value reached (flip case), that's understood because the empty area is function of Dc^2 and the body area (drag) is function of Dc times the constant slice thickness (see figure 3), therefore that this promote that the fluids pass going through the robot and consequently the total drag force be effectad. All of these factors make the reason why the C_D variation has a peculiar performance.

Finally, if we want to improve the drag efficiency we must improve the Columbus design increasing the area ratio more than 50%, an idea could be try to fill the empty area with a kind of flexible metallic membrane.

8. Conclusions

8.1. In partly boundary media, the drag coefficients are dramatically increased by the skin drag and, if the viscous fluids are used the skin drag must be considered upon the total drag effect as the more important factor.

8.2. The instability of the particles appears when d ≥ 0.75D, which means that the velocity U_1 (annular), is increased 16 times U_o and by the Bernoulli equation, the pressure on the particle body is reduced asymmetrically, and the horizontal waving start to rise the particle with out flow variation.

8.3. We could observe the hydrodynamic variations between two vertical positions. For the higher position, the equilibrium velocity is less than the lower position. The boundary layer growing could attribute this phenomenon.

8.4. In order to maximize the C_D coefficients, rings to center the particles has to be added.

8.5. In partly boundary media, the skin drag plays an important roll upon the total drag force as was found with the flip robot. We found a maximum C_D (12%) flipped the Columbus robot.

Finally, if we want to improve the drag efficiency we must improve the Columbus design increasing the area ratio more than 50%, an idea could be try to fill the empty area with a kind of flexible metallic membrane.